Negative regulation of plastidial isoprenoid pathway by herbivore-induced β-cyclocitral in *Arabidopsis thaliana*

Sirsha Mitra[a,b,1], Roger Estrada-Tejedor[c], Daniel C. Volke[d], Michael A. Phillips[e], Jonathan Gershenzon[a], and Louwrance P. Wright[a,1]

[a]Department of Biochemistry, Max Planck Institute for Chemical Ecology, 07745 Jena, Germany; [b]Department of Botany, Savitribai Phule Pune University, Pune-411007, India; [c]Pharmaceutical Chemistry Group, IQS School of Engineering, Universitat Ramon Llull, 08017 Barcelona, Spain; [d]The Novo Nordisk Foundation Center for Biosustainability, Technical University of Denmark, 2800 Kongens Lyngby, Denmark; and [e]Department of Biology, University of Toronto Mississauga, Mississauga, ON L5L 1C6, Canada

Edited by Rodney B. Croteau, Washington State University, Pullman, WA, and approved January 20, 2021 (received for review May 4, 2020)

Insect damage to plants is known to up-regulate defense and down-regulate growth processes. While there are frequent reports about up-regulation of defense signaling and production of defense metabolites in response to herbivory, much less is understood about the mechanisms by which growth and carbon assimilation are down-regulated. Here we demonstrate that insect herbivory down-regulates the 2-C-methyl-D-erythritol-4-phosphate (MEP) pathway in *Arabidopsis* (*Arabidopsis thaliana*), a pathway making primarily metabolites for use in photosynthesis. Simulated feeding by the generalist herbivore *Spodoptera littoralis* suppressed flux through the MEP pathway and decreased steady-state levels of the intermediate 1-deoxy-D-xylulose 5-phosphate (DXP). Simulated herbivory also increased reactive oxygen species content which caused the conversion of β-carotene to β-cyclocitral (βCC). This volatile oxidation product affected the MEP pathway by directly inhibiting DXP synthase (DXS), the rate-controlling enzyme of the MEP pathway in *Arabidopsis* and inducing plant resistance against *S. littoralis*. βCC inhibited both *DXS* transcript accumulation and DXS activity. Molecular models suggested that βCC binds to DXS at the binding site for the thymine pyrophosphate cofactor and blocks catalysis, which was confirmed by direct assays of βCC with the purified DXS protein in vitro. Another intermediate of the MEP pathway, 2-C-methyl-D-erythritol-2, 4-cyclodiphosphate, which is known to stimulate salicylate defense signaling, showed greater accumulation and enhanced export out of the plastid in response to simulated herbivory. Together, our work implicates βCC as a signal of herbivore damage in *Arabidopsis* that increases defense and decreases flux through the MEP pathway, a pathway involved in growth and carbon assimilation.

apocarotenoids | isoprenoid | mechanical damage | methylerythritol-4-phosphate pathway | simulated herbivory

When attacked by herbivores, plants react by generating a variety of chemical signals to induce local and systemic defense responses. Early signaling events include Ca^{2+} influx which depolarizes the cell membrane (1). Elevated Ca^{2+} together with calcium-dependent protein kinases increases the accumulation of membrane-localized NADPH oxidase and leads to the accumulation of reactive oxygen species (ROS) (2). ROS include peroxides, superoxides, hydroxyl radicals, and singlet oxygen ($^1O_2$). $^1O_2$ is a strong electrophile that oxidizes different classes of biomolecules (3). Chloroplasts initiate ROS-dependent stress signaling in response to herbivory (4). In addition, to counteract the detrimental effects of ROS, chloroplasts synthesize antioxidant compounds, including carotenoids, which quench $^1O_2$ (5).

Carotenoids belong to the isoprenoids, a major family of plant metabolites involved in defense and defense signaling. All isoprenoids are derived from isopentenyl diphosphate (IDP) and its isomer dimethylallyl diphosphate (DMADP). Plants use two independent pathways to synthesize IDP and DMADP. One is the cytosolic mevalonate (MVA) pathway that produces IDP and DMADP from acetyl-CoA and provides precursors for sterols, dolichols, sesquiterpenes, and other cytosolic and peroxisomal isoprenoids (6). The remaining plant isoprenoids are synthesized through the plastid-localized 2-*C*-methyl-D-erythritol-4-phosphate (MEP) pathway that synthesizes IDP and DMADP from pyruvate and D-glyceraldehyde 3-phosphate (GAP) (7–9). The MVA pathway is the only source of isoprenoid precursors in animal cells (10), and so its metabolic regulation is generally well understood, partly due to its close relationship with coronary disease in humans (11). In contrast, our understanding of the regulation of the MEP pathway is still in an early stage.

The MEP pathway (Fig. 1) starts with the synthesis of 1-deoxy-D-xylulose-5-phosphate (DXP), catalyzed by 1-deoxy-D-xylulose 5-phosphate synthase (DXS) from pyruvate and GAP (12, 13). In the second step, DXP reductoisomerase (DXR) transforms DXP to MEP. A cytidyl moiety is then introduced to C4 of MEP via a diphosphate bridge to produce 4-(cytidine 5′-diphospho)-2-*C*-methyl-D-erythritol (CDP-ME), catalyzed by MEP-cytidyltransferase (MCT). In the next step, CDP-ME is phosphorylated at C2 by CDP-ME kinase (CMK) to form CDP-ME-2-phosphate

Significance

Plants are known to respond to insect herbivory in multiple ways. Under herbivore attack, plants increase their commitment to defense but decrease their commitment to growth and carbon assimilation. Unfortunately, this second aspect is less studied. Here we report the discovery of an herbivore-triggered signal (β-cyclocitral) that enhances plant resistance and down-regulates the methylerythritol-4-phosphate (MEP) pathway of terpenoid biosynthesis. The MEP pathway supplies the precursors for many metabolites important in photosynthesis such as chlorophylls, carotenoids, plastoquinones, phylloquinones, and tocopherols. We also elucidated the mechanism responsible for the reduction of MEP pathway flux under herbivory and found that β-cyclocitral inhibits the activity of the first step of the pathway, which was also shown to control flux under normal growth conditions.

Author contributions: S.M., J.G., and L.P.W. designed research; S.M., R.E.-T., and D.C.V. performed research; S.M., R.E.-T., and D.C.V. analyzed data; and S.M., R.E.-T., M.A.P., J.G., and L.P.W. wrote the paper.

The authors declare no competing interest.

This article is a PNAS Direct Submission.

[1]To whom correspondence may be addressed. Email: smitra@unipune.ac.in or lwright@tutanota.com.

This article contains supporting information online at https://www.pnas.org/lookup/suppl/doi:10.1073/pnas.2008747118/-/DCSupplemental.

Published March 4, 2021.

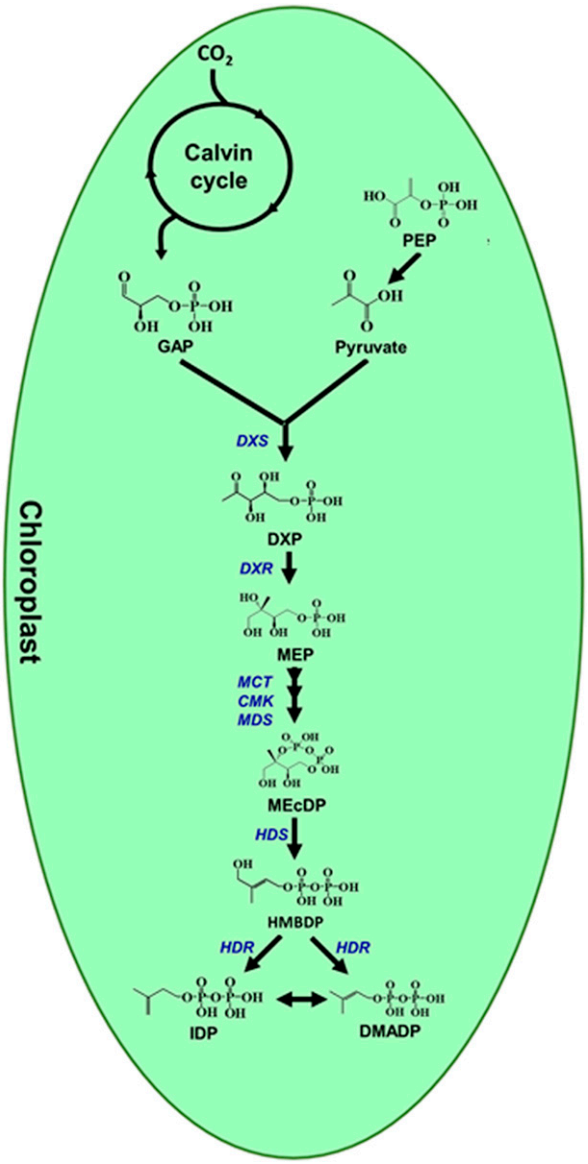

Fig. 1. Outline of the MEP pathway. Intermediates: GAP, D-glyceraldehyde 3-phosphate; PEP, phosphoenol pyruvate; DXP, 1-deoxy-D-xylulose 5-phosphate; MEP, 2-C-methyl-D-erythritol 4-phosphate; MEcDP, 2-C-methyl-D-erythritol-2,4-cyclodiphosphate; HMBDP, 1-hydroxy-2-methyl-2-(*E*)-butenyl 4-diphosphate; IDP, isopentyl diphosphate; and DMADP, dimethylallyl diphosphate. Enzymes: DXS, 1-deoxy-D-xylulose 5-phosphate synthase; DXR, 1-deoxy-D-xylulose 5-phosphate reductase; MCT, MEP cytidylyltransferase; CMK, 4-(cytidine-5′-diphospho)-2-C-methyl-D-erythritol kinase; MDS, MEcDP synthase; HDS, HMBDP synthase; and HDR, HMBDP reductase.

(CDP-MEP). CDP-MEP is then cyclized after loss of the cytidyl group to produce 2-*C*-methyl-D-erythritol-2, 4-cyclodiphosphate (MEcDP), an intermediate that may accumulate under certain conditions (14, 15). MEcDP, which is formed by MEcDP synthase (MDS), is then reduced in the final steps to IDP and DMADP by 1-hydroxy-2-methyl-(*E*)-butenyl 4-diphosphate (HMBDP) synthase (HDS) and HMBDP reductase (HDR). The first step of the pathway, DXS, was recently demonstrated to control the flux through the MEP pathway in photosynthetic tissue of *Arabidopsis thaliana* (*Arabidopsis*) under normal growth conditions despite the fact that its product is sometimes present at a higher steady-state concentration than other measured pathway intermediates (16).

The *A. thaliana* genome encodes one *DXS* gene (*At*4g15560) and two *DXS*-like genes of currently unknown function (*DXL1*, *At*3g21500 and *DXL2, At*5g11380) (17). The accumulation of isoprenoid end products such as carotenoids, chlorophyll *a* and *b*, and tocopherols is sensitive to up- or down-regulation of DXS activity in transgenic plants (18). DXS may be regulated at the transcriptional level (19–21) or through substrate supply (22). Negative feedback can also occur via IDP or DMADP which compete with thiamine pyrophosphate (TPP) at the DXS co-factor binding site (23). This feedback mechanism has been described in poplar but is presumably less important in *Arabidopsis* because IDP and DMADP levels are much lower (16).

The MEP pathway is influenced by different forms of abiotic stress such as high light (24, 25), drought (22), and mechanical wounding (26, 27). However, little is known about the effect of herbivory although *Spodoptera exigua* feeding was shown to suppress DXS and DXR transcript accumulation in *Medicago truncatula* (28). After being wounded or attacked by herbivores, plants typically induce defense responses by activating the jasmonic acid (JA) signaling network (29, 30). However, defense signals can also arise from the MEP pathway. For example, the intermediate MEcDP is a well-known retrograde (plastid-to-nucleus) signal that elicits specific stress genes (31) and other defense responses (32, 33), but its precise role is still not well understood. The volatile isoprene, an immediate product of the MEP pathway, deters the larvae of tobacco hornworm from feeding on tobacco plants (34), perhaps also as a defense signal.

Herbivory not only signals the induction of plant antiherbivore defenses but also causes the suppression of photosynthetic activity beyond what might be predicted from the loss of photosynthetically active surface area (35). Such suppression may act to divert resources from growth or photosynthesis to defense at a time when the plant is threatened by further herbivory (36). However, very little is known about the mobile signals that orchestrate resource allocation after herbivory. Recently, short-chain volatiles have been reported as modulators of defense responses. For example, (*E*)-2-hexenal and (*E*)-2-butenal induce the expression of abiotic stress–related transcription factors in *Arabidopsis*, while the apocarotenoid α-ionone induces resistance against thrips in tomato and *Arabidopsis* (37, 38). Here we report the activity of the cyclic apocarotenoid β-cyclocitral (βCC), an oxidation product of β-carotene elevated after herbivory, increasing defense and suppressing flux through the MEP pathway in *Arabidopsis*. βCC inhibits the MEP pathway by down-regulating DXS activity through decreasing *DXS* transcript levels and direct inhibition of the enzyme. In addition, herbivory causes increased abundance and export of another MEP pathway intermediate, MEcDP, which also stimulates defense.

Results

Wounding and Simulated Herbivory Decrease Photosynthetic Rate. Herbivory has been reported to specifically reduce the levels of gene transcripts and proteins related to photosynthesis (39, 40). Therefore, we began by determining the effect of herbivory on photosynthetic rate in *Arabidopsis* using the leaves of rosette stage wild-type plants that were wounded with a fabric pattern wheel and treated with *Spodoptera littoralis* oral secretion or with sterile water as a control (Fig. 2*A*). Photosynthetic rates were measured under three conditions: in wounded plants treated with oral secretions (simulated herbivory), in wounded plants treated with water (mechanical wounding), and in untreated plants. Simulated herbivory was used instead of actual herbivores to reduce variation and allow for a precise experimental time course (41). Photosynthetic rates in simulated herbivory– and mechanical wounding–treated plants declined significantly over a three-hour period compared with those of untreated plants, declining by 17 to 20% (simulated herbivory) and 20 to 25%

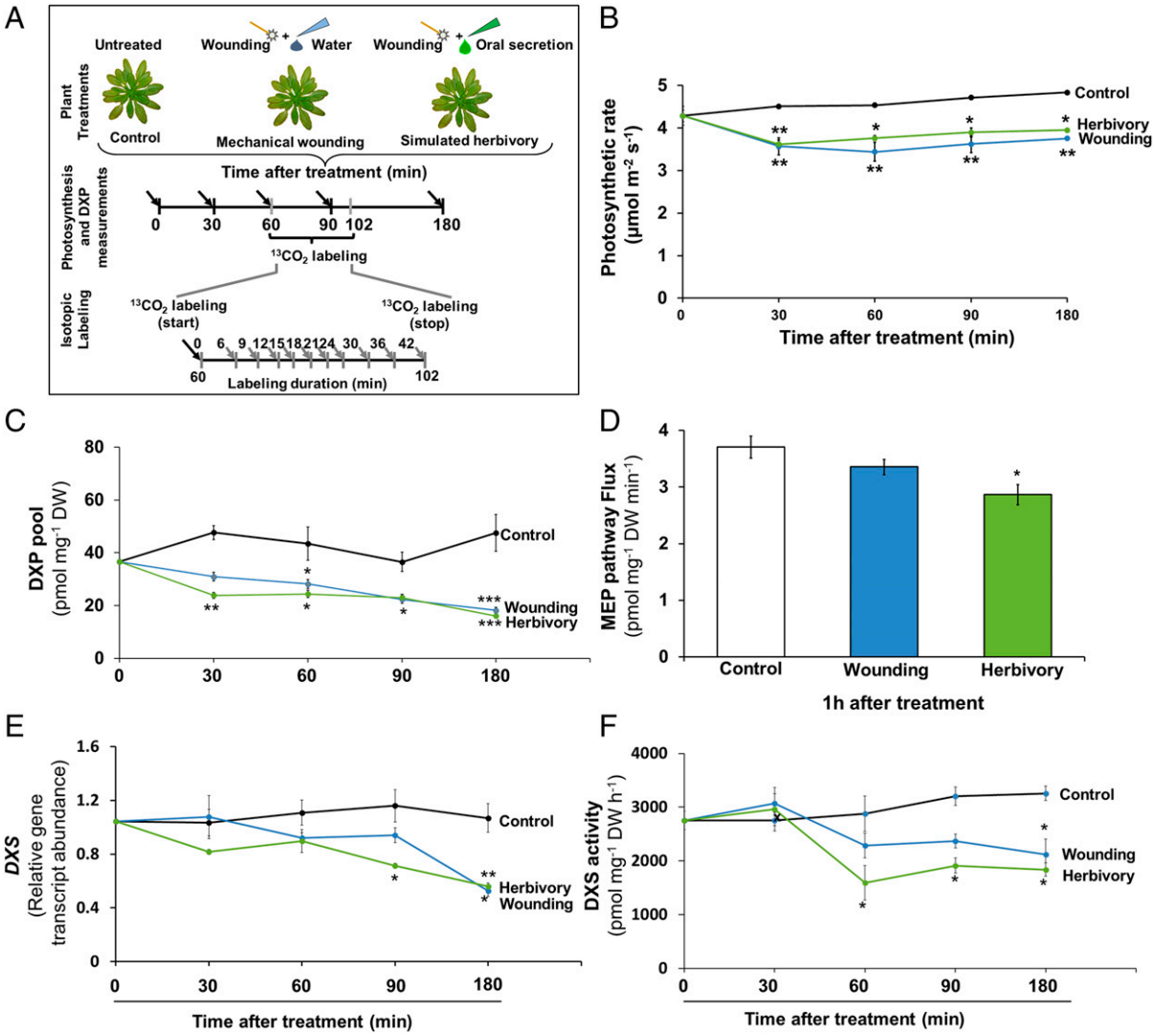

Fig. 2. Mechanical wounding and simulated herbivory decrease photosynthetic rate, DXP pool size, steady-state flux through the MEP pathway, transcript abundance, and activity of DXP synthase, the first step of the MEP pathway in *A. thaliana*. (*A*) Experimental outline showing treatments, timing of measurements, and tissue harvest. Rosette stage *A. thaliana* plants were wounded with a fabric pattern wheel and treated with either sterile water or oral secretion from *S. littoralis* larvae. Photosynthetic rate was measured 30, 60, 90, and 180 min after the experiment began. A second set of similarly treated plants were harvested 30, 60, 90, and 180 min after the experiment began for DXP pool measurement; untreated plants served as controls. For $^{13}CO_2$ labeling, plants were treated as mentioned previously; 60 min after treatment, plants were labeled with $^{13}CO_2$ for 6, 12, 15, 18, 21, 24, 30, 36, or 42 min. Gray arrows signify harvesting time. Black arrows signify photosynthesis and DXP pool measurement times. (*B*) Mechanical wounding (wounding) and simulated herbivory (herbivory) significantly reduced photosynthetic rate compared to untreated plants (two-way ANOVA; $F_{(treatment\times time)\ 2,30} = 2.619$; $P = 0.026$). (*C*) Mechanical wounding and simulated herbivory reduced DXP pool size as compared to untreated plants (two-way ANOVA; $F_{(treatment\times time)\ 2,30} = 5.23$; $P = 0.0003$). (*D*) MEP pathway flux was significantly reduced after simulated herbivory as compared to untreated or mechanically wounded plants (one-way ANOVA; $F_{2,27} = 6.733$; $P = 0.004$; $P_{untreated\ vs.\ W+OS} = 0.003$). Transcript level of DXS and enzyme activity of DXS were measured 30, 60, 90, and 180 min after mechanical wounding and simulated herbivory treatment on rosette stage *A. thaliana* plants and compared with that of untreated plants. (*E*) *DXS* transcript accumulation (two-way ANOVA; $F_{(treatment\times time)\ 2,30} = 3.32$; $P = 0.007$) and (*F*) DXS activity (two-way ANOVA; $F_{(treatment\times time)\ 2,30} = 3.58$; $P = 0.004$) were significantly reduced at various time points after treatment as compared to untreated plants. Values are means (± SE) of three replicate plants for DXP pool size, DXS relative transcript abundance, and DXS activity and 10 replicate plants for flux measurement. Significant differences were determined by two-way ANOVA with Tukey's post hoc test in *B*, *C*, *E*, and *F* and by one-way ANOVA with Tukey's post hoc test in *D*. In two-way ANOVA, since the interaction terms were found to be significant, we refrained from interpreting the main effects of treatment and time. Asterisks indicate significant differences between different treatments at the same time interval at $*P \leq 0.05$; $**P \leq 0.005$; $***P \leq 0.0005$.

(mechanical wounding) (Fig. 2*B*). No change was observed in untreated plants over this same period.

Wounding and Simulated Herbivory Reduce DXP Concentration by Decreasing the Enzyme Activity of DXP Synthase and Expression of the Corresponding Gene. DXP, the first intermediate of the MEP pathway, is formed from the condensation of pyruvate and GAP (Fig. 1), both derived from the Calvin–Benson cycle of photosynthetic carbon fixation. Therefore, impaired photosynthesis could directly affect the MEP pathway by restricting the supply of substrates. As mechanical damage and simulated herbivory reduced photosynthetic rate, we measured DXP accumulation 30, 60, 90, and 180 min after simulated herbivory or mechanical wounding to determine the impact of these treatments on the MEP pathway. We found that the DXP level decreased significantly 60 min after mechanical wounding but already at 30 min after simulated herbivory (Fig. 2*C*). The maximum decrease in DXP levels was 61% and 65% after 180 min for mechanical wounding– and simulated

herbivory–treated plants, respectively. Therefore, these treatments significantly affect the pool size of the first MEP pathway intermediate.

To determine the impact of mechanical wounding and simulated herbivory on the entire MEP pathway, flux measurements were made one hour after treatment. Flux was measured by labeling with $^{13}CO_2$ since freshly fixed carbon enters the MEP pathway, which is localized in the chloroplast, within minutes in *Arabidopsis* leaves (16). Calculations were performed using ^{13}C incorporation into DXP and the DXP pool size as previously described (16). Although DXP and MEcDP were both readily detected as single intermediates, MEcDP was also shown to occur in a pool outside the pathway; hence, DXP was selected for flux measurements. After simulated herbivory, flux through the MEP pathway decreased by 24.3%, but no significant change was elicited by mechanical wounding (Fig. 2*D*). These results suggest that mechanical damage alone was sufficient to reduce photosynthetic rate and DXP pool size but insufficient to reduce flux through MEP pathway, whereas herbivore damage caused declines in all three parameters.

Herbivory triggers large-scale transcriptional changes in many plant species (42, 43), and so we investigated whether transcriptional regulation might be responsible for the metabolic effects we observed. Decreases of nearly 50% in *DXS* transcripts were found for the mechanical wounding and simulated herbivory treatments relative to unwounded controls 3 h following treatment, and significant decreases were evident at even earlier time points for the simulated herbivory treatment (Fig. 2*E*). DXS enzyme activity measured in crude plant extracts was reduced 60 min after simulated herbivory and remained decreased throughout all time points measured for this treatment (Fig. 2*F*). Mechanical wounding decreased DXS activity significantly only at the 3 h time point.

Wounding and Simulated Herbivory Increase MEcDP Levels and Cause Export from the Chloroplast. Abiotic stress has been reported to alter both MEP pathway flux and the concentration of pathway intermediates (25, 31), but the effect of herbivory on these metabolic parameters is unknown. Following the results for DXP, we examined the effect of simulated herbivory on the pool sizes of several other MEP pathway intermediates: MEcDP and IDP+DMADP (measured together) at 0, 30, 60, 90, and 180 min following the above-described treatments or controls. The MEcDP concentration was 30 to 40% higher after 90 and 180 min in both mechanical wounding– and simulated herbivory–treated plants as compared to control plants (Fig. 3*A*), while the level of IDP+DMADP was largely unaltered after these treatments except for a slight reduction 90 min after simulated herbivory (Fig. 3*B*).

Previous studies suggest that levels of MEcDP could build up under oxidative stress because the downstream enzyme, HDS, is highly sensitive to ROS. The accumulated MEcDP is then exported from the site of the MEP pathway in the plastid to other parts of the cell resulting in the formation of a substantial extraplastidic pool of MEcDP under certain stress conditions (14, 16, 31). In our study, the plastidic MEcDP pool decreased in size by 18.3% and 26.2% after mechanical wounding and simulated herbivory, respectively, as compared to untreated plants (Fig. 3 *A*, *Inset*). However, the extraplastidic MEcDP pool of mechanically wounded– and simulated herbivory–treated plants contained 7.5 and 9.0 pmol · mg^{-1} dry weight MEcDP, respectively, representing 16.1% and 20.5% of the total cellular MEcDP in these treatments. No MEcDP was detected outside the plastid in untreated plants; given the similar effects of mechanical wounding and herbivory, we infer that wounding alone is sufficient to cause MEcDP export out of the chloroplast.

Mechanical Wounding and Simulated Herbivory Reduce Certain Isoprenoid End Products. The most abundant end products of the MEP pathway are the pigments involved in photosynthesis,

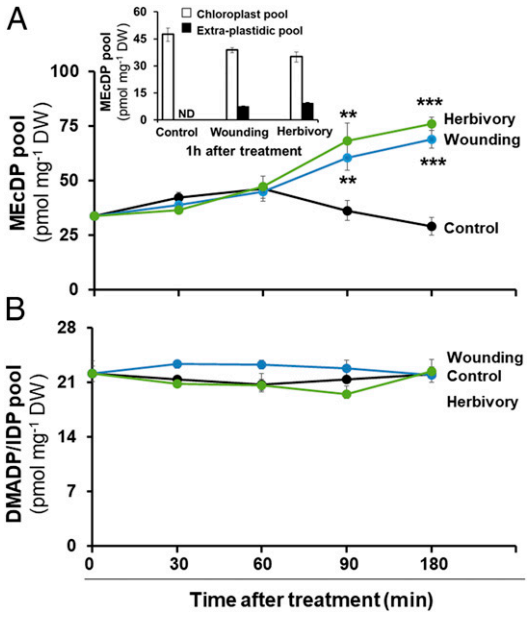

Fig. 3. Mechanical wounding and simulated herbivory increase MEcDP pool size and change its subcellular distribution, while the IDP+DMADP pool is not affected. (*A*) In rosette stage *A. thaliana* plants, mechanical wounding and simulated herbivory substantially increased MEcDP levels (two-way ANOVA; $F_{(treatment\times time)\ 2,30} = 10.54$; $P = 6.769 \times 10^{-7}$) and (*Inset*) increased occurrence in the cytosol vs the chloroplast as compared to untreated plants. Since the interaction terms were found to be significant, we refrained from interpreting the main effects of treatment and time. (*B*) The level of IDP+DMADP slightly decreased 90 min after simulated herbivory but was unchanged at other times and after mechanical wounding (two-way ANOVA; $F_{(treatment\times time)\ 2,30} = 1.4$; $P = 0.2$). As two-way ANOVA showed no significant interaction between treatment and time, we proceeded to interpret the main effects and found that there were significant effects of treatment ($F_{2,30} = 5.94$, $P_{treatment} = 0.006$) but no significant effects of time ($F_{2,30} = 0.775$, $P_{time} = 0.55$). Values are means (± SE) of three replicate plants for MEcDP and IDP+DMADP pool measurement and 10 replicate plants for chloroplast and cytosol MEcDP measurement. Asterisks indicate a significant difference at $P \leq 0.05$ by two-way ANOVA with Tukey's post hoc test. Wounding, mechanical wounding; herbivory, simulated herbivory; and ND, not detected.

namely, chlorophylls (side chain is MEP pathway derived) and carotenoids. The latter are C_{40} primary metabolites with important roles in photosynthesis and protection against ROS. Carotenoids are participants in the xanthophyll cycle that protect plant cells against oxidative stress generated by factors such as an excess of light, drought, chilling, heat, senescence, or salinity stress. Therefore, we measured the levels of the xanthophyll cycle carotenoids neoxanthin and violaxanthin as well as their precursor β-carotene and chlorophyll *a* and *b* after mechanical wounding and simulated herbivory treatments (Fig. 4*A*). Carotenoid levels generally declined after both mechanical wounding and simulated herbivory as compared to untreated plants over the three-hour time course measured (Fig. 4 *B–D*). For example, the level of β-carotene dropped by up to 40% (Fig. 4*B*) while the levels of violaxanthin and neoxanthin displayed decreases of 30 to 80% depending on time point and treatment (Fig. 4 *C* and *D*). Meanwhile, the levels of chlorophyll *a* and *b* decreased by 15 to 30%. (Fig. 4 *E* and *F*).

Reduced β-Carotene Levels in Plants Treated by Mechanical Wounding and Simulated Herbivory Are the Result of Its Oxidation. The levels of β-carotene declined ~40% within 30 min after wounding and simulated herbivory, but it seemed unlikely that these decreases were a result of reductions in the supply of MEP pathway precursors since pathway flux declined at a substantially lower rate

over the same time span. In many plant species, wounding and herbivory elicit the production of ROS (44–49), such as $^1O_2$, which are known to cause rapid oxidation of carotenoids (50) (Fig. 5*A*). We therefore hypothesized that simulated herbivory–induced $^1O_2$ had degraded β-carotene and analyzed the accumulation of total ROS using the 2′ 7′-dichlorofluorescein diacetate (DCFDA) assay. We found ROS accumulation to be ∼3-fold higher in mechanically wounded plants after 90 min in comparison to untreated controls (Fig. 5*B*) Consistent with our other observations, simulated herbivory produced similar effects, but on a shorter time scale (i.e., a threefold increase in ROS after 60 min) (Fig. 5*B*).

Since the DCFDA assay does not identify the ROS involved, we monitored the transcript accumulation of $^1O_2$ and H_2O_2 marker genes. We saw a two- to threefold induction of two $^1O_2$ responsive genes, Touch (*AtTCH4*) and BON2-associated protein 1(*AtBAP1*), at early time points (Fig. 5 *E* and *F*). Expression of a marker gene encoding an H_2O_2-responsive gene (*AtHP1*: At1g49150) (50) remained unaltered at the early time points (Fig. 5*E*), increasing only 180 min after mechanical wounding and simulated herbivory treatment (Fig. 5*G*). These marker gene measurements imply that decreases in β-carotene levels following wounding treatments may be the result of $^1O_2$-catalyzed breakdown.

Oxidation of β-Carotene Forms the Volatile Product βCC. Oxidative cleavage of β-carotene produces a number of volatile apocarotenoids such as βCC and β-ionone (βI) (50). βCC has previously been proposed as a stress signal that is sensitive to $^1O_2$. Based on the apparent generation of $^1O_2$ and observed reduction in β-carotene under our treatment regimes, we next measured βCC and βI accumulation. In control plants, βCC and βI were detected at ∼60 and 50 ng · g^{-1} FW, respectively. However, βCC rose by about 25% 90 min after mechanical wounding and increased nearly 35% in only 30 min after simulated herbivory (Fig. 5*F*), maintaining this level through the last time point sampled. On the other hand, the level of βI increased by 63% at 60 min after mechanical wounding but remained unaltered after simulated herbivory treatments as compared to untreated plants (Fig. 5*G*). Based on these observations, we further investigated the role of βCC in regulating flux through the MEP pathway.

βCC Application Decreases Pool Sizes of MEP Pathway Intermediates In Vivo. The possibility that βCC down-regulates the MEP pathway (Fig. 6*A*), it was evaluated by measuring the concentration of MEP pathway metabolites in plants treated with different concentrations of βCC or water as a control. We found that DXP, MEcDP, and IDP+DMADP levels all decreased following exogenous βCC treatment (Fig. 6 *B–D*). We found a negative correlation between the level of MEP pathway intermediates and βCC concentration. When βCC treatment was coupled with mechanical wounding or simulated herbivory, decreases in DXP were even more pronounced than plants treated with βCC alone (*SI Appendix*, Fig. S1). This additive effect indicates that herbivory-induced βCC negatively regulates the accumulation of DXP. MEcDP concentration decreased significantly when βCC treatment was coupled with simulated herbivory treatment, but there was no effect when βCC was coupled with mechanical

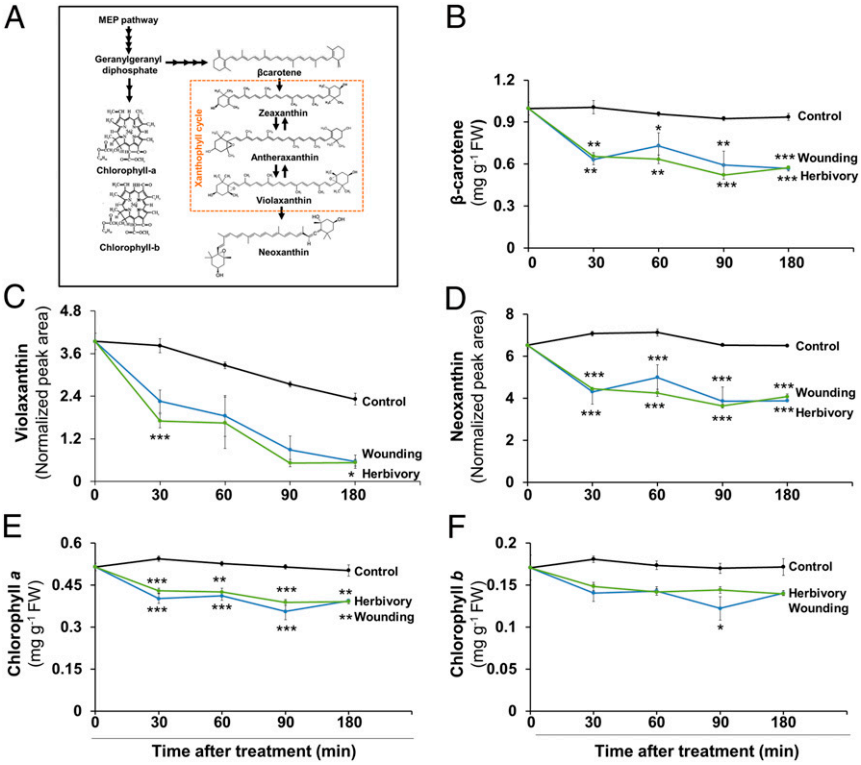

Fig. 4. Mechanical wounding and simulated herbivory decrease accumulation of photosynthetic pigments. (*A*) Outline of metabolic connections between MEP pathway and photosynthetic pigment biosynthesis. Rosette stage *A. thaliana* plants were wounded with a fabric pattern wheel and treated with either sterile water or oral secretion from *S. littoralis* larvae and the accumulation of pigments were measured. The levels of carotenoids, namely, (*B*) β-carotene (two-way ANOVA; $F_{(\text{treatment}\times\text{ time})\ 2,30} = 4.2$; $P = 0.001$), (*C*) violaxanthin (two-way ANOVA; $F_{(\text{treatment}\times\text{time})\ 2,30} = 1.6$; $P = 0.14$; $F_{(\text{treatment})\ 2,30} = 23.99$; $P = 5.978 \times 10^{-7}$; $F_{(\text{time})\ 2,30} = 33.15$; $P = 1.293 \times 10^{-10}$), (*D*) neoxanthin (two-way ANOVA; $F_{(\text{treatment}\times\text{time})\ 2,30} = 7.46$; $P = 1.939 \times 10^{-5}$), and (*E*) chlorophyll *a* (two-way ANOVA; $F_{(\text{treatment}\times\text{time})\ 2,30} = 5.74$; $P = 0.0001$) were significantly decreased after mechanical wounding (wounding) and simulated herbivory (herbivory) treatments. However, the levels of (*F*) chlorophyll *b* were decreased only 90 min after mechanical wounding (wounding) (two-way ANOVA; $F_{(\text{treatment}\times\text{time})\ 2,30} = 1.2$; $P = 0.29$; $F_{(\text{treatment})\ 2,30} = 15.7$; $P = 2.158 \times 10^{-05}$; $F_{(\text{time})\ 2,30} = 3.42$; $P = 0.02$). Values are means (± SE) of three replicate plants. Asterisks indicate significant difference at $P \leq 0.05$ by two-way ANOVA with Tukey's post hoc test.

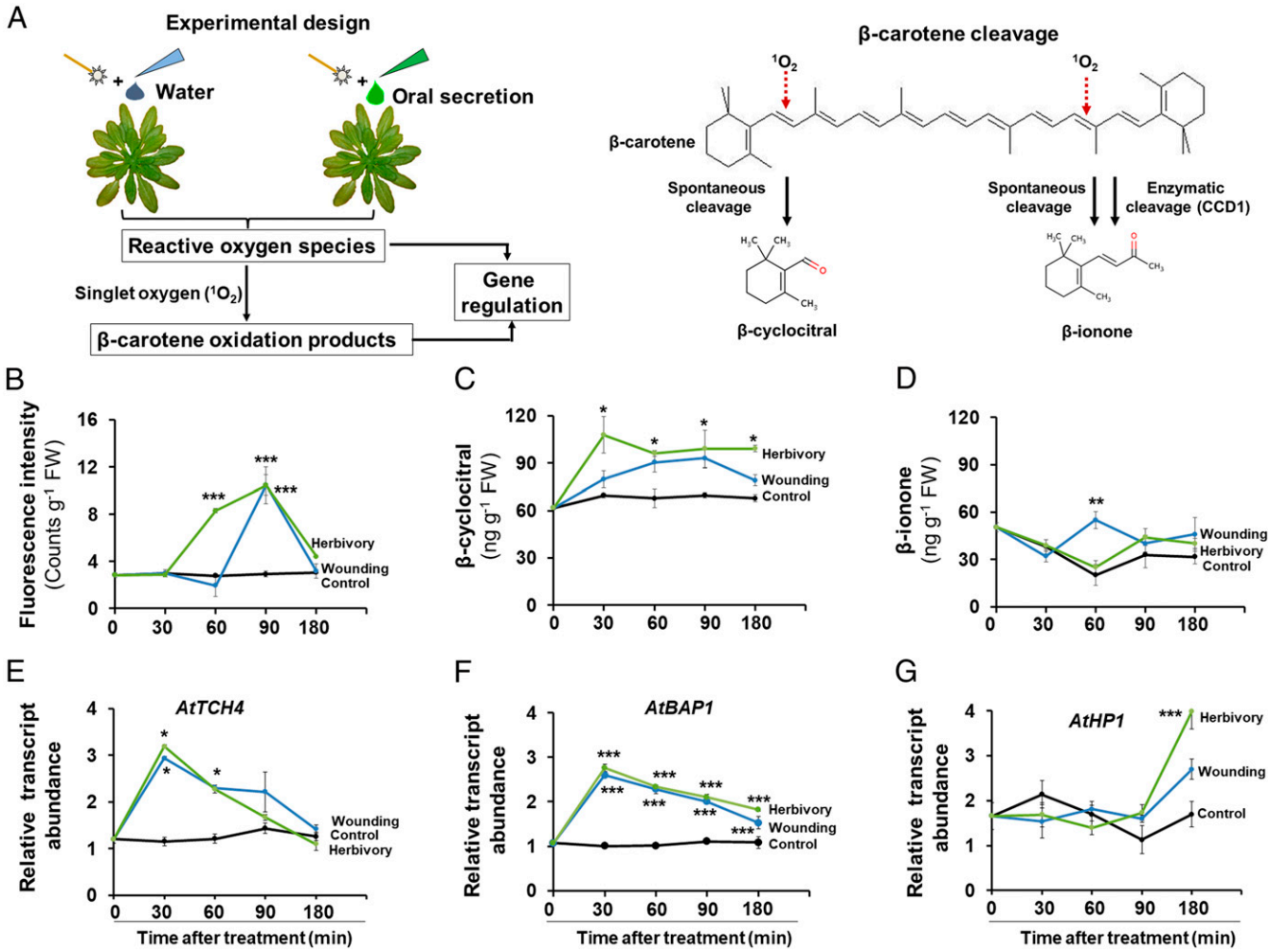

Fig. 5. Mechanical wounding and simulated herbivory oxidize β-carotene and increase the accumulation of βCC. (*A*) Schematic showing the hypothesis that $^1O_2$ arising from mechanical wounding (wounding) and simulated herbivory (herbivory) imposed by mechanical wounding and addition of insect oral secretion causes oxidation of β-carotene and accumulation of βCC. (*B*) Accumulation of ROS was increased 90 min after mechanical wounding and 60 min after simulated herbivory (two-way ANOVA; $F_{(\text{treatment}\times\text{time})\ 2,30} = 16.54$; $P = 4.641 \times 10^{-9}$). Of the two major β-carotene oxidation products measured, the level of (*C*) βCC was significantly increased after simulated herbivory (two-way ANOVA; $F_{(\text{treatment}\times\text{time})\ 2,30} = 2.46$; $P = 0.03$), but the level of (*D*) βI was not (two-way ANOVA; $F_{(\text{treatment}\times\text{time})\ 2,30} = 4.02$; $P = 0.002$). The expression of the $^1O_2$ marker genes (*E*) *AtTCH4* (two-way ANOVA; $F_{(\text{treatment}\times\text{time})\ 2,30} = 4.36$; $P = 0.001$) and (*F*) *AtBAP1* were significantly increased 30 min after mechanical wounding and simulated herbivory treatment (two-way ANOVA; $F_{(\text{treatment}\times\text{time})\ 2,30} = 26.82$; $P = 1.213 \times 10^{-11}$); however, the expression of the H_2O_2 marker gene (*G*) *AtHP1* was significantly increased only 180 min after mechanical wounding and simulated herbivory treatment (two-way ANOVA; $F_{(\text{treatment}\times\text{time})\ 2,30} = 5.7$; $P = 0.0001$). Values are means (± SE) of three replicate plants for fluorescence and gene expression analysis and four replicate plants for βCC and βI analysis. Asterisks indicate a significant difference at $P \leq 0.05$ by two-way ANOVA with Tukey's post hoc test.

wounding or applied to untreated plants (*SI Appendix*, Fig. S1). From these observations, we conclude that βCC application specifically targets DXP levels.

βCC Down-Regulates *DXS* Transcript Accumulation and DXS Enzyme Activity. To reveal how βCC causes a drop in DXP pool size, we examined the transcript accumulation and activity of DXS as well as the overall photosynthetic rate in *A. thaliana* plants after exposure to βCC. We found that the photosynthetic rate remained unaltered in βCC-treated plants as compared to water controls (Fig. 6*E*). However, the transcript level of *DXS* and activity of DXS were reduced in βCC-treated plants as compared to controls (Fig. 6 *F* and *G*), decreasing by up to 25% and 50%, respectively.

In the MEP pathway, MDS is responsible for the formation of MEcDP, and then HDS and HDR sequentially convert MEcDP to IDP and DMADP (17). Transcriptional control of the genes encoding these downstream pathway enzymes could produce the observed changes in MEcDP and IDP+DMADP levels in βCC-treated plants. However, transcript levels of *MDS*, *HDS*, and *HDR* did not change upon βCC application (Fig. 6 *H–J*) as *DXS* did in a manner commensurate with the metabolite changes (Fig. 6 *B–D*). Therefore, we conclude that βCC treatment specifically affects the levels of *DXS* transcripts and not the transcripts for genes encoding these downstream steps of the MEP pathway.

βCC Inhibits DXS Catalysis Based on the Results of Molecular Modeling and In Vitro Assays. The potential for direct interaction between DXS and βCC was first evaluated by molecular modeling. While no three-dimensional structure is available for *A. thaliana* DXS, the crystal structure of *Escherichia coli* DXS has been published with a resolution of 2.4 Å. Using the *E. coli* structure, we predicted the molecular structure of *A. thaliana* DXS dimer (*At*DXS) by homology modeling and inserted the cofactor TPP into the catalytic site (*SI Appendix*, Fig. S3). The possible binding sites of TPP were first evaluated computationally (*SI Appendix*, Fig. S4*A*). The alpha triangle algorithm was

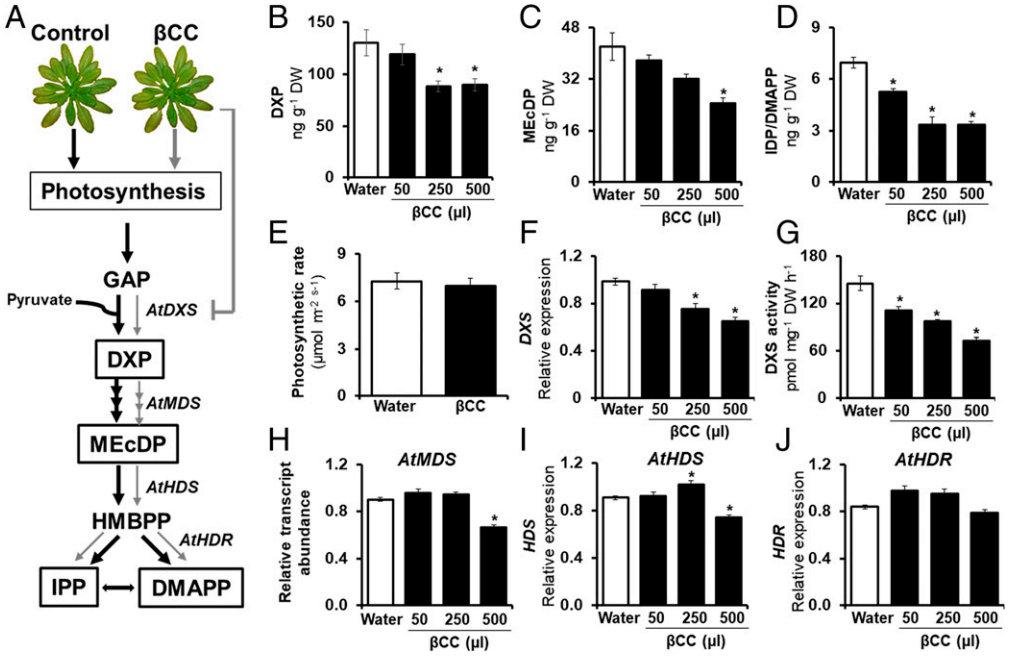

Fig. 6. βCC down-regulates the MEP pathway by decreasing accumulation of pathway intermediates, *DXS* transcript levels, and DXS enzyme activity. (*A*) Schematic showing the hypothesis that βCC negatively regulates the accumulation of MEP pathway intermediates by reducing DXS activity but not photosynthesis. Depicted are the major intermediates of the MEP pathway, DXP, MEcDP, and IDP/DMADP, and the genes encoding the enzymes that produce them, *DXS*, *MDS*, *HDS*, and *HDR*. Arrows qualitatively depict the flux conditions following treatment of βCC (gray) or water (black) as a control. Thicknesses of the arrows are proportional to the level of metabolites. βCC treatment significantly decreased the accumulation of the intermediates (*B*) DXP (one-way ANOVA; $F_{3,12} = 5.548$; $P = 0.012$), (*C*) MEcDP (one-way ANOVA; $F_{3,12} = 9.312$; $P = 0.00185$), and (*D*) IDP/DMADP (Welch's ANOVA; $F_{3,6.362} = 38.74$; $P < 0.00017$). βCC treatment did not alter (*E*) photosynthetic rate [measured under photosynthetically active radiation (PAR) 500 μmol · m^{-2} · s^{-1}, CO_2 concentration 400 μmol · mol^{-1}, and 21 °C] (Student's *t* test; $t_{(7)} = 0.401$; $P = 0.701$). However, βCC treatment significantly reduced both (*F*) *DXS* expression (one-way ANOVA; $F_{3,8} = 17.32$; $P = 0.0007$) and (*G*) DXS activity (one-way ANOVA; $F_{3,12} = 29.02$; $P < 0.0001$). Levels of (*H*) *MDS* (one-way ANOVA; $F_{3,12} = 36.24$; $P < 0.0001$), (*I*) *HDS* (one-way ANOVA; $F_{3,12} = 20.25$; $P < 0.0001$), and (*J*) *HDR* (one-way ANOVA; $F_{3,12} = 6.927$; $P = 0.0058$) transcripts were not correlated with the accumulation patterns of MEcDP and IDP/DMADP. Values are means (± SE) of three replicate plants for *F* and four replicate plants for all others. Asterisks indicate significant difference at $P \leq 0.05$ by one-way ANOVA or Welch's test with Tukey's post hoc test.

used in the blind docking process for the placement of 200 interacting conformations (500,000 iterations for each pose) using London dG as the scoring function. The best 100 conformations were refined and their binding energy estimated by the GBVI/WSA dG scoring function. The resulting conformations could be grouped into eight main clusters (*SI Appendix*, Fig. S4*B*). As expected, conformations with highest affinity values corresponded to binding pockets abutting the dimer interface which would not be accessible to the ligand and so were not further considered. The interactions between the *At*DXS–TPP complex and ligands (the substrate pyruvate and the potential inhibitor βCC) were then predicted by flexible protein docking. Both ligands were able to interact in the active site previously described, abutting the TPP cofactor, and stabilize their pose by hydrogen bonding with Tyr472. However, the molecular stability of the protein–ligand complexes, as assessed by molecular dynamics simulations, suggested a difference between pyruvate and βCC interaction. βCC altered the local stabilization of Tyr368 leading to the blockage of the active site (Fig. 7 *A–D*).

To confirm the results of the molecular modeling, the inhibition of βCC was tested directly in an in vitro assay with heterologously expressed and purified *A. thaliana* DXS. The K_m values for pyruvate (158 μM), GAP (27 μM), and TPP (35 μM) were determined first and these concentrations used for the βCC inhibition assays. The activity of DXS was then found to be reduced by increasing concentrations of βCC (Fig. 7*E*). When mean values were fitted with the equation y = a*x^b with a = 100; +95% confidence interval, the specific βCC concentration that was able to inhibit the activity of DXS by 50% (IC_{50}) was found to be 8 mM. This result suggests that βCC negatively regulates the activity of DXS in planta.

βCC Treatment Reduces Herbivore Performance due to the Induction of Metabolic Changes in the Plant. Since we showed that βCC is induced by herbivory, we examined whether this metabolite might play a role in defense signaling. The performance of a generalist herbivore, *S. littoralis*, was evaluated on βCC-treated plants. *S. littoralis* larvae gained 23% less mass when fed on βCC-treated plants as compared with larvae fed on water-treated controls (Fig. 8*A*). To test if βCC had any direct toxicity or deterrency toward *S. littoralis* larvae, larvae were tested on an artificial diet containing different concentrations of βCC. However, *S. littoralis* larvae gained similar mass when fed on an artificial diet containing βCC or a solvent control (Fig. 8*B*), suggesting that decreased larval performance may be attributed to βCC-mediated metabolic changes in plants rather than the effects of direct ingestion of βCC.

Discussion

Herbivore attack can trigger both the activation of plant defense pathways and the suppression of pathways involved in growth and photosynthesis. In this study, we demonstrated that an herbivore-triggered signal in *Arabidopsis*, βCC, inhibits the first enzyme of the MEP pathway whose major products are photosynthetic pigments. The resulting decrease in flux through the MEP pathway is accompanied by a rise in plant defense capacity against a chewing herbivore (Fig. 9).

Herbivory Decreases Flux through the *Arabidopsis* MEP Pathway via Down-Regulating DXS, the First Step of the Pathway. After herbivory, plants are known to increase their commitment to antiherbivore defenses and decrease their investment in other processes such as growth and carbon assimilation. For example, after being fed upon by *Manduca sexta* larvae, *Nicotiana attenuata* down-regulates the formation of proteins needed for photosynthesis (40). Herbivory on *Arabidopsis* by different herbivorous insects decreased the expression of genes encoding many types of proteins involved in photosynthesis and other pathways of primary metabolism (51). The MEP pathway in *Arabidopsis* could also be down-regulated upon herbivory as its major end products are carotenoids and the prenyl side chain of chlorophylls. Formation of photosynthetic pigments might be expected to have a lower priority than defense after herbivore attack.

To study the effect of herbivory on the MEP pathway in *Arabidopsis*, we first established that simulated herbivory decreased the rate of photosynthesis which occurred within 30 min (Fig. 2). Next, we determined the flux through MEP pathway and levels of DXP, the first intermediate of the pathway. Flux through MEP pathway can be altered by a number of methods including the use of inhibitors that target the first two enzymes of the pathway, namely, DXS and DXR (52). However, the use of inhibitors may interfere with assessing the effects of herbivory. Labeling with stable isotopes allows precise flux measurements, especially when label is supplied to an intact plant from a natural substrate like CO_2 rather than from sugars administered to detached organs (53). Since the products of the MEP pathway form so many different products, determining accurate flux rates would be simplified by measuring the incorporation of isotopic label not into pathway products but into intermediates which can be sensitively measured using liquid chromatography–mass spectrometry (LC-MS) (54). Measuring $^{13}CO_2$ incorporation into pathway intermediates, herbivory was found to decrease flux through the MEP pathway by 25% within 1 h with the first enzyme, DXS, showing reduced activity after herbivory and the corresponding gene having lower transcript levels (Fig. 2). After mechanical damage, on the other hand, DXS activity was not significantly reduced by the same time point. This suggests that though wounding alone can influence DXS, herbivory enhances the effect. Previous studies on the MEP pathway in *Arabidopsis* had shown by metabolic control analysis that DXS had a very high flux control coefficient under normal growth conditions (16), so down-regulation by herbivory would be expected to decrease pathway flux. However, the greater reduction in the DXP pool (44%) as compared to the decrease in flux (25%) suggests that the levels of DXP are decreased by more than just a decline in pathway flux and DXS activity. A reduction in the DXP pool may also result from a decline in substrate supply to the pathway as a result of the decrease in photosynthetic rate.

Herbivore-Induced Signaling of the MEP Pathway Proceeds via a Carotenoid Oxidation Product, βCC. The first hint about the mechanism by which herbivory could inhibit the MEP pathway was the observed decline in a MEP pathway product, β-carotene (Fig. 4*B*), accompanied by an increase in its oxidation product βCC (Fig. 5*C*). Therefore, we hypothesized that herbivore-induced accumulation of βCC is due to degradation of β-carotene. Found in many plant species (55), βCC has been shown to serve as an internal signal regulating root growth (56) and helping plants adjust to oxidative stress caused by high light conditions (50). As a product of carotenoid oxidation by $^1O_2$, it seems a good indicator of oxidative stress and could have many different effects. In fact, βCC treatment of *Arabidopsis* had been demonstrated to reprogram expression of more than 1,000 genes (50). Hence, we examined the effect of βCC on the MEP pathway. Exposure of *Arabidopsis* to βCC led to decreases in MEP pathway intermediate pools (Fig. 6). The decrease in DXP accumulation was ascribed to a decrease in *DXS* transcript accumulation and DXS enzyme activity. Meanwhile, the expression

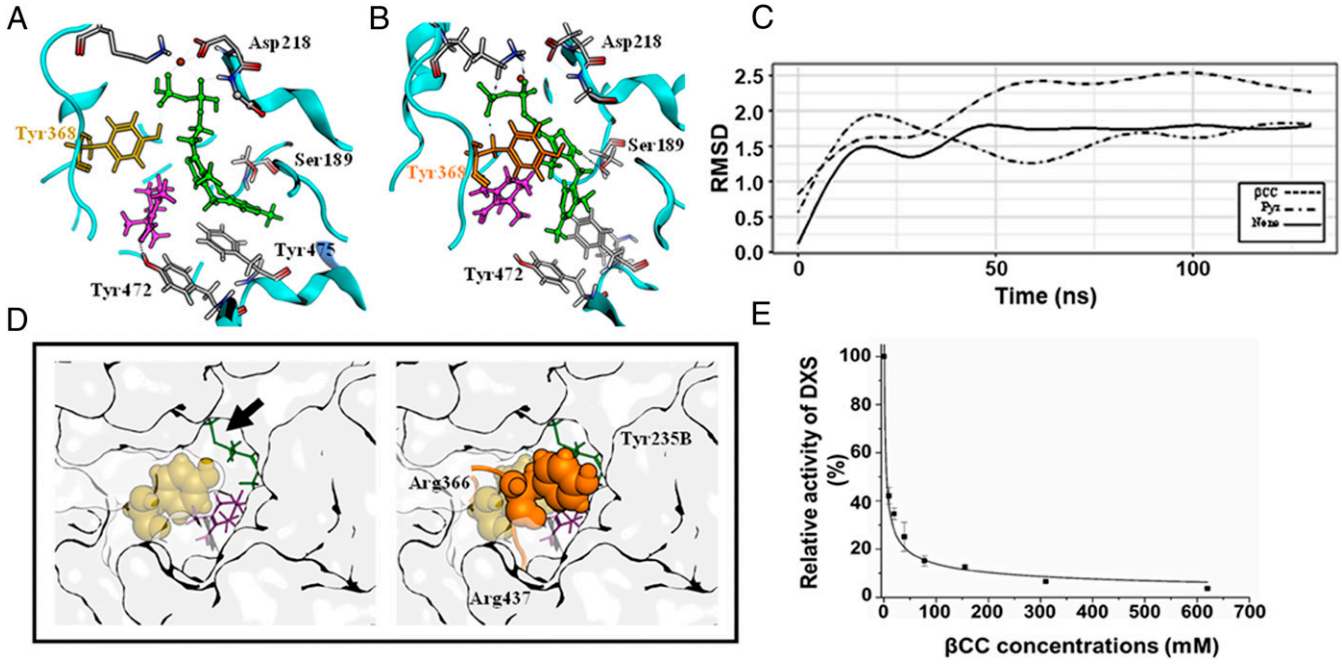

Fig. 7. βCC binds to DXS at the TPP binding site and inhibits DXS activity. (*A*) Binding mechanism predicted by molecular docking suggests that βCC competes for the pyruvate binding site of DXS. (*B*) The mechanism of action of βCC could involve a modification of TPP interactions such that the cofactor no longer binds to Asp218 but is instead pushed toward Ser189. (*C*) rmsd of TPP during molecular dynamics simulations conducted alone, complexed with pyruvate, or complexed with βCC. Higher rmsd values indicate a major change in TPP position. (*D*) The main effect of βCC on DXS structure results in the modification of Tyr368, which blocks the entrance to the active site. (*E*) BCC inhibits DXS activity in an in vitro assay with heterologously expressed and purified DXS. The IC_{50} value for βCC is 8 mM. Data points are means (± SE) of three technical replicates.

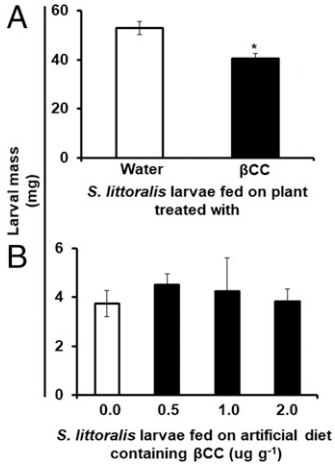

Fig. 8. *S. littoralis* larval growth was reduced when fed on βCC-treated plants but not on βCC-supplemented artificial diet. *S. littoralis* larval mass gain was recorded after 12 d of feeding on βCC-treated *A. thaliana* (~40-d-old) plants and on artificial diet containing βCC dissolved in MeOH. Larvae fed on water-treated plants or on artificial diet that was supplemented with MeOH were used as respective controls. (*A*) Mass of *S. littoralis* larvae was significantly decreased when fed on βCC-treated plants as compared to water-treated plants (Student's *t* test; $t_{(28)}$= 3.634; P = 0.0011). Values are means (± SE) of 15 replicate larvae. The asterisk indicates significant difference at $P \leq 0.05$ by Student's *t* test. (*B*) *S. littoralis* larval mass did not change significantly when fed on artificial diet supplemented with βCC as compared to control (one-way ANOVA; $F_{3,24}$ = 0.296; P = 0.828). Values are means (± SE) of seven replicate larvae.

of other MEP pathway genes and the rate of photosynthesis were not affected by βCC treatment. The impact of βCC on DXS fits with this apocarotenoid serving as a signal in herbivore-triggered down-regulation of the MEP pathway, which we had already demonstrated to occur via suppression of DXS activity. Down-regulation of the MEP pathway over the longer term should eventually reduce the supply of carotenoids and chlorophylls.

The formation of βCC from β-carotene could result from the action of carotenoid cleavage dioxygenases (CCD) which cleave β-carotene at specific sites and produce βCC and other apocarotenoids (57–59). However, previous work (50) had shown that the level of βCC did not change in *Arabidopsis* CCD mutants. Photo-oxidation of β-carotene triggered by $^1O_2$ is known to produce βCC as well as other carotenoids such as βI and dihydroactinidiolide (50). We measured a sharp rise in ROS following herbivory, which could be attributed to $^1O_2$ by changes in marker gene expression (Fig. 5). Thus $^1O_2$-driven oxidation of β-carotene is likely responsible for the βCC produced on herbivory.

βCC Inhibits DXS Catalysis by Binding at the TPP-Binding Site. As an α,β-unsaturated aldehyde, βCC might act directly on DXS or another protein because of its reactivity with nucleophilic moieties such as sulfhydryl groups. Electrophiles with α,β-unsaturated carbonyl functions have been previously implicated in plant signaling processes (60, 61). Meanwhile, DXS itself is a protein known to be influenced by the binding of small ligands. In addition to the TPP cofactor, the MEP intermediates IDP and DMADP are reported to be feedback inhibitors of DXS in *Populus trichocarpa* (23). IDP and DMADP both compete with TPP for binding to the protein. Given that βCC application reduces DXS activity in planta, we applied a molecular modeling approach to determine if this volatile apocarotenoid might also bind to DXS. Interaction mechanisms predicted by molecular docking for pyruvate and βCC suggested a similar binding site for both molecules involving interaction with Tyr472. This residue corresponds to Tyr392 in *E.coli* DXS (identified through sequence alignment), which has been described as a key residue for pyruvate binding (62). Molecular dynamics simulations revealed that βCC also had an impact on the position of TPP as well as on the structure of the DXS protein. During the simulation, βCC pushed TPP against the back pocket away from its catalytic position to Ser189 where the pyruvate binds (Fig. 7*B*), a change not observed when simulating the DXS–TPP complex without βCC or in presence of pyruvate (Fig. 7*C*). As a consequence of the new position of TPP, the geometry of some residues was modified, particularly Tyr368, so that the entrance to the active site became blocked. Our results therefore indicated that βCC can bind to DXS and inhibit its catalysis by blocking the active site (Fig. 7*A*). Hence βCC has the potential to profoundly influence DXS activity in planta and so could regulate MEP pathway flux.

Further evidence for βCC inhibition of DXS came from direct assay with the heterologously expressed *A. thaliana* protein in which βCC reduced DXS activity in vitro. While the IC_{50} value of 8 mM indicates only weak inhibition, the lipophilicity and volatility of this ligand make it hard to judge its effective concentration in experimental settings. To investigate the in vivo role of βCC in more detail, future efforts should be made to measure

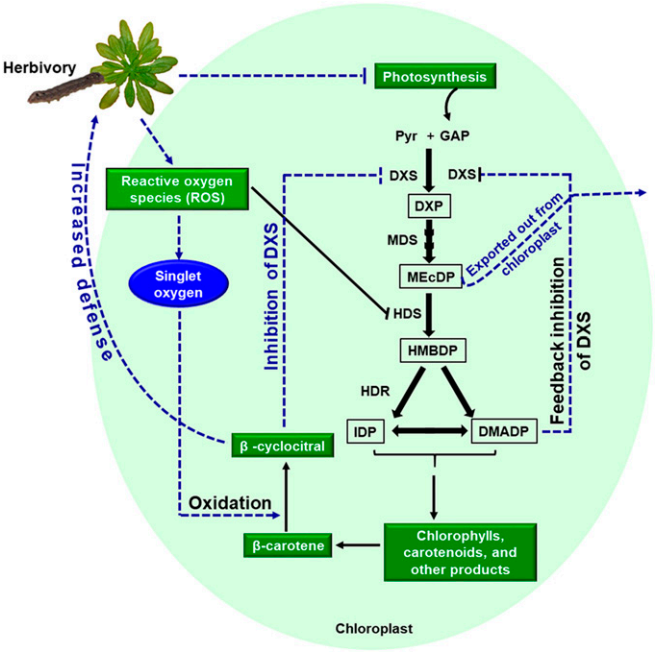

Fig. 9. Scheme for down-regulation of MEP pathway in *Arabidopsis* by insect herbivory. Herbivory decreases photosynthesis and triggers an increase in ROS accumulation. Among ROS, $^1O_2$ then converts β-carotene to the oxidation product βCC. In turn, βCC inhibits DXS, the rate-controlling enzyme of the MEP pathway. In previous work, the end products of the pathway, IDP and DMADP, have also been shown to inhibit DXS activity (23). In addition to down-regulating the MEP pathway, which is involved in growth and development, βCC also triggers increased defense against herbivores. Moreover, the ROS induced by herbivory also induces another defense response via the MEP pathway. ROS stimulate a build-up of the intermediate MEcDP due to inhibition of the ROS-sensitive enzyme immediately following. The accumulated MEcDP is then transported out of the chloroplast and into the nucleus where it has been shown to stimulate the expression of defense genes (31). Black solid arrows indicate metabolic conversions. Blue dashed lines indicate regulatory effects, positive with an arrowhead and negative with an inhibition bar. Intermediates: DMADP, dimethylallyl diphosphate; DXP, 1-deoxy-D-xylulose 5-phosphate; GAP, D-glyceraldehyde 3-phosphate; HMBDP, 1-hydroxy-2-methyl-2-(*E*)-butenyl 4-diphosphate; IDP, isopentenyl diphosphate; MEcDP, 2-C-methyl-D-erythritol-2,4-cyclodiphosphate; and Pyr, pyruvate. Enzymes: DXS, DXP synthase; HDR, HMBDP reductase; HDS, HMBDP synthase; and MDS, MEcDP synthase.

the concentration present upon herbivory in the chloroplast, the site of the MEP pathway, and to determine the mode of inhibition caused by βCC.

Herbivory-Induced Increase in MEcDP Leads to a Comprehensive Defense Response against Different Types of Herbivores. Unlike DXP, another later intermediate of the MEP pathway, MEcDP, increased after herbivory and was exported from the site of the pathway in the plastid to the cytosol (Fig. 3). In previous $^{13}CO_2$ labeling experiments, MEcDP was shown to form a pool outside the plastids that was labeled with different kinetics than pools of other intermediates that remain in the plastids (16). Such an extraplastidial pool was also described in *Arabidopsis* mutants blocked in the next pathway step, HDS (63) (Fig. 1), and in lines overexpressing the rate-limiting enzyme DXS (16). In our study, the increase of MEcDP after herbivory may be attributed to the effect of herbivory-generated ROS on HDS, an enzyme with an Fe–S cluster that is quite sensitive to ROS (64). Significant reduction of HDS activity could lead to a build-up of MEcDP even when overall pathway flux is reduced, particularly if this intermediate is exported away from the site of the pathway where it can no longer be used up in later steps. The level of MEcDP is affected in a different way after βCC treatment in the absence of herbivory. Here, MEP pathway flux is expected to decline, but since no increase in ROS was observed (*SI Appendix*, Fig. S5), HDS and HDR would be expected to maintain their activity so MEcDP should not accumulate. This is indeed the case (Fig. 6) arguing for the ROS sensitivity of downstream enzymes being responsible for the build-up of MEcDP.

Extraplastidial MEcDP is well established as the source of a plastid-to-nucleus signal that up-regulates salicylic acid (SA) signaling (31, 32). This enhancement of SA signaling by MEcDP export from the plastid has been demonstrated to increase the resistance of *Arabidopsis* to phloem-feeding insects, such as the cabbage aphid *Brevicoryne brassicae*, but does not decrease JA signaling, contrary to the typical antagonistic SA–JA crosstalk frequently reported in *Arabidopsis* (33). In the present study, we showed that simulated lepidopteran herbivory increased the defensive posture of *Arabidopsis* to a leaf-chewing herbivore, the larvae of *S. littoralis*, via βCC signaling (Fig. 7). This simulated herbivory treatment likely also enhanced SA signaling and triggered defenses against phloem-feeding herbivores since we detected an increase in export of MEcDP from the plastid, although we did not measure SA or conduct assays with aphids in this study. The end result of both βCC and MEcDP signaling is thus a multitiered defense response to different kinds of herbivores more comprehensive than simple induction of either SA or JA signaling by itself. Further research is needed to determine how βCC and MEcDP signaling interact with other defense signaling cascades.

Herbivore-Triggered Suppression of the MEP Pathway Facilitates Increased Allocation to Antiherbivore Defenses. Whatever the mechanism, the down-regulation of the MEP pathway by herbivory may be part of plant strategy to divert resources from growth and carbon assimilation toward defense after herbivore attack. The MEP pathway in *Arabidopsis* leaves is principally involved in making metabolites for photosynthesis including the carotenoid and chlorophyll pigments, the antioxidant tocopherols, and the prenylquinone electron carriers. The components of the photosynthetic machinery should be in lower demand after herbivore damage, since herbivory commonly decreases the rate of photosynthesis via decreases in the levels of gene transcripts encoding proteins related to photosynthesis (39, 40). Herbivore-induced decreases in MEP pathway flux will free resources for other purposes including defense. Plants commonly exhibit trade-offs between growth and defense (36), which is frequently explained as a result of limited resources that constrain their ability to maximize all functions simultaneously. However, recent research suggests that the balance between growth and defense is not a direct result of limited supplies of fixed carbon, energy, and other resources. Rather, plants prioritize one process over another under specific environmental conditions as regulated by a complex signaling network (65). In our study, under conditions of herbivore attack, *Arabidopsis* employed a βCC-driven signaling network to suppress the MEP pathway, a nondefense process. We also found βCC to trigger an increase in plant defense against *S. littoralis* larvae (Fig. 7). Although we did not investigate which specific defenses were activated, βCC treatment of *Arabidopsis* has previously been shown to activate genes encoding trypsin proteinase inhibitors and enzymes involved in flavonoid glycoside formation (50). *Arabidopsis* trypsin inhibitors are reported to confer defense against spider mites (66), while elevated levels of glycosylated flavonoids in *Arabidopsis* are known to reduce the growth of *Pieris brassicae* larvae (67). There are numerous reports on herbivore induction of plant defenses in *Arabidopsis* (68) and many other plant species (69), but much less is known about how herbivory down-regulates the processes of growth and assimilation. In addition to the MEP pathway, future research is likely to discover many other primary metabolic pathways to be modulated by herbivory. In addition to damping growth, herbivory may also promote storage of plant resources for increased survival under stress. In fact, βCC, which we showed to be induced by herbivory, was just recently demonstrated to enhance root growth and branching in *Arabidopsis* by promoting cell division in root meristems (56). This may help plants to store additional carbohydrates and other resources in roots which may be allocated to this organ after herbivory (70).

Our findings on βCC's ability to down-regulate the MEP pathway have practical implications since though the pathway is present in many bacteria, protozoa, and plants, it is absent in humans. Therefore, substances that disrupt the MEP pathway could find use as herbicides or antibacterial and antiprotozoan drugs. For example, fosmidomycin, a compound isolated from some *Streptomyces* species that inhibits the activity of DXP reductoisomerase (the second step of the pathway), has potential as an antimalarial compound (71, 72). The synthetic compound ketoclomazone, which inhibits DXS, shows antibacterial activity against *Haemophilus influenza* (73). Since we showed that βCC could inhibit the whole MEP pathway, this apocarotenoid could also be a candidate for herbicide or drug development.

Materials and Methods

Plant Material, Growth Conditions, and Treatments. *A. thaliana* (Columbia, Col-0 accession) plants were grown under short-day (10 h light/14 h dark) conditions at 21 °C and 140 μmol · m^{-2} · s^{-1} PPFD for 5 wk. Rosette stage plants 36 to 40 d old were used for all experiments. Plants were wounded with a fabric pattern wheel and treated with 80 μL sterile distilled water for the mechanical wounding treatment or oral secretion of *S. littoralis* (diluted with 1 vol water) for the simulated herbivory treatment. Plants were harvested 0, 30, 60, 90, and 180 min after the treatment with untreated plants used as controls. Harvested tissues were stored at −80 °C until further use and used for all the time series analysis. To investigate the effect of βCC, plants were placed in a 3-L glass desiccator under the same growth conditions for 4 h. Each desiccator contained two plants. Different amounts of pure βCC (50 μL, 250 μL, and 500 μL) were deposited on a watch glass placed inside the desiccator. Water was used as a control as described (50). Tissues were harvested immediately after 4 h of the βCC treatment and stored at −80 °C until further use.

Photosynthetic Rate, $^{13}CO_2$ Labeling, and Flux Analysis. A LI-6400XT Portable Photosynthesis System (Li-Cor Biosciences) was used together with a custom-built *Arabidopsis* cuvette (74) to measure the photosynthetic rate and to perform in vivo $^{13}CO_2$ labeling as described in ref. 16.

Flux through the MEP pathway was calculated from the absolute ^{13}C incorporation into DXP in time course labeling assays ranging from 6 to 42 min in untreated, mechanical wounding–treated, or simulated herbivory–treated plants. Prior to $^{13}CO_2$ labeling, plants were adapted in the gas exchange cuvette in a normal atmosphere with an airflow of 500 L · min^{-1} for ∼30 min to achieve a photosynthetic steady state. For each treatment, 10 individual

plants were labeled in time course experiments. The total labeled fraction of DXP was calculated as previously described (16).

Extraction of Plant Metabolites. Lyophilized and pulverized plant material (5 mg) was extracted for analysis of MEP pathway intermediates as previously described (16). The procedure for the analysis of β-carotene and its oxidation products is provided in *SI Appendix*.

LC-MS/MS Analysis of MEP Pathway Intermediates. MEP pathway intermediates, including the level of ^{13}C incorporation in DXP and MEcPP were analyzed on an Agilent 1260 HPLC system (Agilent Technologies) connected to an API 5000 triple quadrupole mass spectrometer (AB Sciex). The experimental details for the separation of MEP pathway intermediates are provided in the *SI Appendix*.

High-Performance Liquid Chromatography Analysis of Carotenoids and Oxidation Products. β-Carotene analysis was accomplished using an Agilent 1100 HPLC system equipped with a diode array detector. For separation of pigments, a Supelcosil LC-18 column (3-μm particle size, length × inner diameter: 75 × 4.6 mm) and for separation of the two major β-carotene oxidation products, βCC and βI, an Agilent XDB-C18 column (1.8 μm, 4.6 mm × 50 mm) was used. The mobile phases for β-carotene and its oxidation products are described in the *SI Appendix*.

RNA Isolation, cDNA Synthesis, and Quantitative RT-PCR. Total RNA was extracted from rosette stage plants using the RNeasy plant mini kit (Qiagen) using buffer RLT according to the manufacturer's instructions. Complementary DNA (cDNA) was synthesized from 0.5 mg total RNA using SuperScript III reverse transcriptase (Invitrogen, Thermo Fisher). Quantitative RT-PCR was performed by using the Mx3500P (Stratagene) system and gene-specific primer pairs (*SI Appendix*, Table S1). Adenine phosphoribosyltransferase 1 (AT1G27450) was used as a reference gene to normalize cDNA concentration. Transcript fold change was calculated using the primer efficiency method. All target and reference gene reactions were performed in three or four technical replicates.

DXS Enzyme Assay. DXS activity was measured in total protein extracts from untreated, mechanically wounded, and simulated herbivory *A. thaliana* rosette plants. Harvested tissues were lyophilized, and 5 mg lyophilized tissue was used for protein extraction. Extraction buffer and assay buffer were prepared as described (16, 75). The procedure for protein extraction, enzyme assay, and product quantification are provided in *SI Appendix*.

Determination of ROS by Fluorescence. Total ROS was determined by a modified 2′, 7′ DCFDA (Sigma Aldrich) assay as described (76). The procedure is provided in *SI Appendix*.

Computational Modeling of *A. thaliana* DXS. The three-dimensional structure of the *A. thaliana* DXS dimer was predicted by homology modeling. The structure of the *E. coli* DXS protein reported in the Protein Data Bank (PDB ID: 2O1S) (77) was used as a template and the *At*DXS sequence was retrieved from Uniprot (ID: Q38854). Sequence alignment, homology modeling, and de novo modeling of unresolved loops were conducted using Molecular Operating Environment (MOE) 2019.01 software (Chemical Computing Group Inc.). The TPP cofactor was initially placed in the *At*DXS model obtained by analogy to the binding mechanism described for the *E. coli* DXS and it was energy minimized, keeping the protein atoms fixed. The resulting model was therefore refined by molecular dynamics simulations (*SI Appendix*, Fig. S3). Since no prior information about the βCC binding site was available, the most likely pocket was initially assessed by blind docking. Results suggested that βCC preferably binds DXS near the catalytic site. For this reason, the binding mechanisms for pyruvate and βCC were predicted by flexible docking against the catalytic binding site using the MOE software. Both ligands were docked against the TPP binding site using Triangle Matcher function for placement and the GBVI/WSA dG scoring function to estimate the binding affinity. The docking protocols were validated by reproducing the TPP binding mechanism described in *E. coli* DXS (rmsd < 2Å). Since the active site is immediately adjacent to the dimer interface, all calculations consider the *At*DXS in its dimeric form.

The procedure for molecular dynamics simulations is provided in *SI Appendix*.

Heterologous Expression of DXS and In Vitro Assay with βCC. DXS from *A. thaliana* was cloned into the pET41a vector (*SI Appendix*, Fig. S6), and the resulting plasmids were used for expression in *E. coli* BL21 under standard expression conditions (78) yielding ∼5 mg of *At*DXS from 1 L Luria–Bertani medium. The protein was expressed with an N-terminal GST-tag and purified by ammonium sulfate precipitation followed by glutathione affinity chromatography.

DXS activity was measured in 50 mM Tris HCl, pH 8.0 with 10 mM $MgCl_2$ at 37 °C. Assays were carried out in a total volume of 100 μL and started with the addition of 0.1 μg enzyme. The reaction was carried out under linear conditions and stopped after 10 min by the addition of 400 μl quenching solution (1:1, methanol: acetonitrile). DXP in the samples was quantified following the method described under LC-MS/MS analysis of MEP pathway intermediates. Finally, the curve was fitted with a power function and the IC_{50} of βCC was calculated.

Herbivore Performance on βCC-Treated Plants. Rosette stage *A. thaliana* were treated with water or βCC for 4 h in a glass desiccator and allowed to stand for 1 h. Freshly hatched *S. littoralis* larvae were then transferred to βCC- or water-treated plants and allowed to feed for 12 d. Plants were replaced every day with similarly treated plants.

Statistical Analysis. Data were analyzed with SPSS (version 17.0; SPSS Inc.), Stat View (Abacus Concepts Inc.), and PAST 3 (version 3.22) freeware for Microsoft Windows. All quantitative data were analyzed by Student's *t* test, one-way ANOVA, Welch's test, and two-way ANOVA. Statistical significance was determined using a Tukey's honest significant difference or a Games Howell post hoc test. Origin 8.5 pro was used to fit the DXS enzyme inhibition data.

Data Availability. All study data are included in the article and/or *SI Appendix*.

ACKNOWLEDGMENTS. We thank Dr. M. Reichelt for help with the LC-MS analysis, the Max Planck Institute for Chemical Ecology glasshouse team for growing the plants, Mrs. B. Raguschke for technical assistance, and Dr. S. Dey for useful discussions and suggestions. This work was supported by a Max Planck Society and Fraunhofer Institute Cooperation grant and a Ramalingaswami Re-entry Fellowship from the Department of Biotechnology, Ministry of Science and Technology, India.

1. G. Arimura, M. E. Maffei, Calcium and secondary CPK signaling in plants in response to herbivore attack. *Biochem. Biophys. Res. Commun.* **400**, 455–460 (2010).
2. J. Wu, I. T. Baldwin, Herbivory-induced signalling in plants: Perception and action. *Plant Cell Environ.* **32**, 1161–1174 (2009).
3. C. Triantaphylidès, M. Havaux, Singlet oxygen in plants: Production, detoxification and signaling. *Trends Plant Sci.* **14**, 219–228 (2009).
4. G. Bonaventure, I. T. Baldwin, New insights into the early biochemical activation of jasmonic acid biosynthesis in leaves. *Plant Signal. Behav.* **5**, 287–289 (2010).
5. F. Ramel *et al*., Chemical quenching of singlet oxygen by carotenoids in plants. *Plant Physiol.* **158**, 1267–1278 (2012).
6. A. Hemmerlin, J. L. Harwood, T. J. Bach, A raison d'être for two distinct pathways in the early steps of plant isoprenoid biosynthesis? *Prog. Lipid Res.* **51**, 95–148 (2012).
7. M. Rohmer, M. Knani, P. Simonin, B. Sutter, H. Sahm, Isoprenoid biosynthesis in bacteria: A novel pathway for the early steps leading to isopentenyl diphosphate. *Biochem. J.* **295**, 517–524 (1993).
8. W. Eisenreich *et al*., The deoxyxylulose phosphate pathway of terpenoid biosynthesis in plants and microorganisms. *Chem. Biol.* **5**, R221–R233 (1998).
9. E. Cordoba, M. Salmi, P. León, Unravelling the regulatory mechanisms that modulate the MEP pathway in higher plants. *J. Exp. Bot.* **60**, 2933–2943 (2009).
10. J. L. Goldstein, M. S. Brown, Regulation of the mevalonate pathway. *Nature* **343**, 425–430 (1990).
11. A. Endo, The discovery and development of HMG-CoA reductase inhibitors. *J. Lipid Res.* **33**, 1569–1582 (1992).
12. B. M. Lange, M. R. Wildung, D. McCaskill, R. Croteau, A family of transketolases that directs isoprenoid biosynthesis via a mevalonate-independent pathway. *Proc. Natl. Acad. Sci. U.S.A.* **95**, 2100–2104 (1998).
13. L. M. Lois *et al*., Cloning and characterization of a gene from Escherichia coli encoding a transketolase-like enzyme that catalyzes the synthesis of D-1-deoxyxylulose 5-phosphate, a common precursor for isoprenoid, thiamin, and pyridoxol biosynthesis. *Proc. Natl. Acad. Sci. U.S.A.* **95**, 2105–2110 (1998).
14. D. González-Cabanelas *et al*., The diversion of 2-C-methyl-D-erythritol-2,4-cyclodiphosphate from the 2-C-methyl-D-erythritol 4-phosphate pathway to hemiterpene glycosides mediates stress responses in *Arabidopsis thaliana*. *Plant J.* **82**, 122–137 (2015).
15. C. Rivasseau *et al*., Accumulation of 2-C-methyl-D-erythritol 2,4-cyclodiphosphate in illuminated plant leaves at supraoptimal temperatures reveals a bottleneck of the prokaryotic methylerythritol 4-phosphate pathway of isoprenoid biosynthesis. *Plant Cell Environ.* **32**, 82–92 (2009).

16. L. P. Wright *et al*., Deoxyxylulose 5-phosphate synthase controls flux through the methylerythritol 4-phosphate pathway in Arabidopsis. *Plant Physiol.* **165**, 1488–1504 (2014).
17. M. A. Phillips, P. León, A. Boronat, M. Rodríguez-Concepción, The plastidial MEP pathway: Unified nomenclature and resources. *Trends Plant Sci.* **13**, 619–623 (2008).
18. J. M. Estévez, A. Cantero, A. Reindl, S. Reichler, P. León, 1-Deoxy-D-xylulose-5-phosphate synthase, a limiting enzyme for plastidic isoprenoid biosynthesis in plants. *J. Biol. Chem.* **276**, 22901–22909 (2001).
19. E. Cordoba *et al*., Functional characterization of the three genes encoding 1-deoxy-D-xylulose 5-phosphate synthase in maize. *J. Exp. Bot.* **62**, 2023–2038 (2011).
20. M. A. Phillips *et al*., Functional identification and differential expression of 1-deoxy-D-xylulose 5-phosphate synthase in induced terpenoid resin formation of Norway spruce (*Picea abies*). *Plant Mol. Biol.* **65**, 243–257 (2007).
21. M. Saladié, L. P. Wright, J. Garcia-Mas, M. Rodriguez-Concepcion, M. A. Phillips, The 2-C-methylerythritol 4-phosphate pathway in melon is regulated by specialized isoforms for the first and last steps. *J. Exp. Bot.* **65**, 5077–5092 (2014).
22. F. Brilli *et al*., Response of isoprene emission and carbon metabolism to drought in white poplar (*Populus alba*) saplings. *New Phytol.* **175**, 244–254 (2007).
23. A. Banerjee *et al*., Feedback inhibition of deoxy-D-xylulose-5-phosphate synthase regulates the methylerythritol 4-phosphate pathway. *J. Biol. Chem.* **288**, 16926–16936 (2013).
24. G. Mongélard *et al*., Measurement of carbon flux through the MEP pathway for isoprenoid synthesis by (31)P-NMR spectroscopy after specific inhibition of 2-C-methyl-d-erythritol 2,4-cyclodiphosphate reductase. Effect of light and temperature. *Plant Cell Environ.* **34**, 1241–1247 (2011).
25. Z. Li, T. D. Sharkey, Metabolic profiling of the methylerythritol phosphate pathway reveals the source of post-illumination isoprene burst from leaves. *Plant Cell Environ.* **36**, 429–437 (2013).
26. G. Arimura *et al*., Effects of feeding *Spodoptera littoralis* on lima bean leaves: IV. Diurnal and nocturnal damage differentially initiate plant volatile emission. *Plant Physiol.* **146**, 965–973 (2008).
27. S. Bartram, A. Jux, G. Gleixner, W. Boland, Dynamic pathway allocation in early terpenoid biosynthesis of stress-induced lima bean leaves. *Phytochemistry* **67**, 1661–1672 (2006).
28. J. C. Bede, R. O. Musser, G. W. Felton, K. L. Korth, Caterpillar herbivory and salivary enzymes decrease transcript levels of *Medicago truncatula* genes encoding early enzymes in terpenoid biosynthesis. *Plant Mol. Biol.* **60**, 519–531 (2006).
29. C. Wasternack, S. Song, Jasmonates: Biosynthesis, metabolism, and signaling by proteins activating and repressing transcription. *J. Exp. Bot.* **68**, 1303–1321 (2017).
30. A. Mithöfer, W. Boland, Recognition of herbivory-associated molecular patterns. *Plant Physiol.* **146**, 825–831 (2008).
31. Y. Xiao *et al*., Retrograde signaling by the plastidial metabolite MEcPP regulates expression of nuclear stress-response genes. *Cell* **149**, 1525–1535 (2012).
32. M. Lemos *et al*., The plastidial retrograde signal methyl erythritol cyclopyrophosphate is a regulator of salicylic acid and jasmonic acid crosstalk. *J. Exp. Bot.* **67**, 1557–1566 (2016).
33. N. Onkokesung *et al*., The plastidial metabolite 2-C-methyl-D-erythritol-2,4-cyclodiphosphate modulates defence responses against aphids. *Plant Cell Environ.* **42**, 2309–2323 (2019).
34. J. Laothawornkitkul *et al*., Isoprene emissions influence herbivore feeding decisions. *Plant Cell Environ.* **31**, 1410–1415 (2008).
35. A. R. Zangerl *et al*., Impact of folivory on photosynthesis is greater than the sum of its holes. *Proc. Natl. Acad. Sci. U.S.A.* **99**, 1088–1091 (2002).
36. D. A. Herms, W. J. Mattson, The dilemma of plants - to grow or defend. *Q. Rev. Biol.* **67**, 283–335 (1992).
37. Y. Yamauchi, M. Kunishima, M. Mizutani, Y. Sugimoto, Reactive short-chain leaf volatiles act as powerful inducers of abiotic stress-related gene expression. *Sci Rep-Uk*, **5** (2015).
38. M. Murata, T. Kobayashi, S. Seo, alpha-Ionone, an apocarotenoid, induces plant resistance to western flower thrips, *Frankliniella occidentalis*, independently of jasmonic acid. *Molecules* **25**, E17 (2019).
39. R. Halitschke, U. Schittko, G. Pohnert, W. Boland, I. T. Baldwin, Molecular interactions between the specialist herbivore *Manduca sexta* (Lepidoptera, Sphingidae) and its natural host *Nicotiana attenuata*. III. Fatty acid-amino acid conjugates in herbivore oral secretions are necessary and sufficient for herbivore-specific plant responses. *Plant Physiol.* **125**, 711–717 (2001).
40. A. P. Giri *et al*., Molecular interactions between the specialist herbivore *Manduca sexta* (Lepidoptera, Sphingidae) and its natural host *Nicotiana attenuata*. VII. Changes in the plant's proteome. *Plant Physiol.* **142**, 1621–1641 (2006).
41. T. E. Ohnmeiss, I. T. Baldwin, The allometry of nitrogen to growth and an inducible defense under nitrogen-limited growth. *Ecology* **75**, 995–1002 (1994).
42. M. De Vos *et al*., Signal signature and transcriptome changes of Arabidopsis during pathogen and insect attack. *Mol. Plant Microbe Interact.* **18**, 923–937 (2005).
43. A. Kessler, I. T. Baldwin, Plant responses to insect herbivory: The emerging molecular analysis. *Annu. Rev. Plant Biol.* **53**, 299–328 (2002).
44. J. L. Bi, G. W. Felton, Foliar oxidative stress and insect herbivory: Primary compounds, secondary metabolites, and reactive oxygen species as components of induced resistance. *J. Chem. Ecol.* **21**, 1511–1530 (1995).
45. P. J. Jih, Y. C. Chen, S. T. Jeng, Involvement of hydrogen peroxide and nitric oxide in expression of the ipomoelin gene from sweet potato. *Plant Physiol.* **132**, 381–389 (2003).
46. M. Leitner, W. Boland, A. Mithöfer, Direct and indirect defences induced by piercing-sucking and chewing herbivores in *Medicago truncatula*. *New Phytol.* **167**, 597–606 (2005).
47. M. E. Maffei *et al*., Effects of feeding *Spodoptera littoralis* on lima bean leaves. III. Membrane depolarization and involvement of hydrogen peroxide. *Plant Physiol.* **140**, 1022–1035 (2006).
48. M. Orozco-Cardenas, C. A. Ryan, Hydrogen peroxide is generated systemically in plant leaves by wounding and systemin via the octadecanoid pathway. *Proc. Natl. Acad. Sci. U.S.A.* **96**, 6553–6557 (1999).
49. A. Prasad, M. Sedlářová, R. S. Kale, P. Pospíšil, Lipoxygenase in singlet oxygen generation as a response to wounding: In vivo imaging in *Arabidopsis thaliana*. *Sci. Rep.* **7**, 9831 (2017).
50. F. Ramel *et al*., Carotenoid oxidation products are stress signals that mediate gene responses to singlet oxygen in plants. *Proc. Natl. Acad. Sci. U.S.A.* **109**, 5535–5540 (2012).
51. S. Zhou, Y.-R. Lou, V. Tzin, G. Jander, Alteration of plant primary metabolism in response to insect herbivory. *Plant Physiol.* **169**, 1488–1498 (2015).
52. J. Zeidler *et al*., Inhibition of the Non-Mevalonate 1-Deoxy-D-xylulose-5-phosphate pathway of plant isoprenoid biosynthesis by fosmidomycin. *Z. Naturforsch. C* **53**, 980–986 (1998).
53. M. Rohmer, M. Seemann, S. Horbach, S. Bringer-Meyer, H. Sahm, Glyceraldehyde 3-phosphate and pyruvate as precursors of isoprenic units in an alternative non-mevalonate pathway for terpenoid biosynthesis. *J. Am. Chem. Soc.* **118**, 2564–2566 (1996).
54. D. González-Cabanelas, A. Hammerbacher, B. Raguschke, J. Gershenzon, L. P. Wright, Quantifying the metabolites of the methylerythritol 4-phosphate (MEP) pathway in plants and bacteria by liquid chromatography–triple quadrupole mass spectrometry. *Methods Enzymol.* **576**, 225–249 (2016).
55. A. Felemban, J. Braguy, M. D. Zurbriggen, S. Al-Babili, Apocarotenoids involved in plant development and stress response. *Front. Plant Sci.* **10**, 1168 (2019).
56. A. J. Dickinson *et al*., β-Cyclocitral is a conserved root growth regulator. *Proc. Natl. Acad. Sci. U.S.A.* **116**, 10563–10567 (2019).
57. D. S. Floss, M. H. Walter, Role of carotenoid cleavage dioxygenase 1 (CCD1) in apocarotenoid biogenesis revisited. *Plant Signal. Behav.* **4**, 172–175 (2009).
58. F. Bouvier, J. C. Isner, O. Dogbo, B. Camara, Oxidative tailoring of carotenoids: A prospect towards novel functions in plants. *Trends Plant Sci.* **10**, 187–194 (2005).
59. M. J. Rodrigo *et al*., A novel carotenoid cleavage activity involved in the biosynthesis of Citrus fruit-specific apocarotenoid pigments. *J. Exp. Bot.* **64**, 4461–4478 (2013).
60. E. E. Farmer, C. Davoine, Reactive electrophile species. *Curr. Opin. Plant Biol.* **10**, 380–386 (2007).
61. M. J. Mueller, S. Berger, Reactive electrophilic oxylipins: Pattern recognition and signalling. *Phytochemistry* **70**, 1511–1521 (2009).
62. L. A. B. Basta, H. Patel, L. Kakalis, F. Jordan, C. L. F. Meyers, Defining critical residues for substrate binding to 1-deoxy-D-xylulose 5-phosphate synthase–active site substitutions stabilize the predecarboxylation intermediate C2α-lactylthiamin diphosphate. *FEBS J.* **281**, 2820–2837 (2014).
63. M. J. Gil, A. Coego, B. Mauch-Mani, L. Jordá, P. Vera, The Arabidopsis csb3 mutant reveals a regulatory link between salicylic acid-mediated disease resistance and the methyl-erythritol 4-phosphate pathway. *Plant J.* **44**, 155–166 (2005).
64. A. Banerjee, T. D. Sharkey, Methylerythritol 4-phosphate (MEP) pathway metabolic regulation. *Nat. Prod. Rep.* **31**, 1043–1055 (2014).
65. T. Züst, A. A. Agrawal, Trade-offs between plant growth and defense against insect herbivory: An emerging mechanistic synthesis. *Annu. Rev. Plant Biol.* **68**, 513–534 (2017).
66. A. Arnaiz *et al*., Arabidopsis Kunitz trypsin inhibitors in defense against spider mites. *Front. Plant Sci.* **9**, 986 (2018).
67. N. Onkokesung *et al*., Modulation of flavonoid metabolites in Arabidopsis thaliana through overexpression of the MYB75 transcription factor: Role of kaempferol-3,7-dirhamnoside in resistance to the specialist insect herbivore *Pieris brassicae*. *J. Exp. Bot.* **65**, 2203–2217 (2014).
68. S. Textor, J. Gershenzon, Herbivore induction of the glucosinolate–myrosinase defense system: Major trends, biochemical bases and ecological significance. *Phytochem. Rev.* **8**, 149–170 (2009).
69. R. Ray, D. Li, R. Halitschke, I. T. Baldwin, Using natural variation to achieve a whole-plant functional understanding of the responses mediated by jasmonate signaling. *Plant J.* **99**, 414–425 (2019).
70. J. Schwachtje, I. T. Baldwin, Why does herbivore attack reconfigure primary metabolism? *Plant Physiol.* **146**, 845–851 (2008).
71. T. Kuzuyama, T. Shimizu, S. Takahashi, H. Seto, Fosmidomycin, a specific inhibitor of 1-deoxy-D-xylulose 5-phosphate reductoisomerase in the nonmevalonate pathway for terpenoid biosynthesis. *Tetrahedron Lett.* **39**, 7913–7916 (1998).
72. H. Jomaa *et al*., Inhibitors of the nonmevalonate pathway of isoprenoid biosynthesis as antimalarial drugs. *Science* **285**, 1573–1576 (1999).
73. Y. Matsue *et al*., The herbicide ketoclomazone inhibits 1-deoxy-D-xylulose 5-phosphate synthase in the 2-C-methyl-D-erythritol 4-phosphate pathway and shows antibacterial activity against *Haemophilus influenzae*. *J. Antibiot. (Tokyo)* **63**, 583–588 (2010).
74. M. Loivamäki *et al*., Circadian rhythms of isoprene biosynthesis in grey poplar leaves. *Plant Physiol.* **143**, 540–551 (2007).
75. L. Wright, M. A. Phillips, *Measuring the Activity of 1-Deoxy-D-Xylulose 5-phosphate Synthase, the First Enzyme in the MEP Pathway, in Plant Extracts* (Humana Press, Springer, New York, 2014).
76. N. Jambunathan, *Determination and Detection of Reactive Oxygen Species (ROS), Lipid Peroxidation, and Electrolyte Leakage in Plants* (Springer Science+Business Media, LLC, 2010).
77. S. Xiang, G. Usunow, G. Lange, M. Busch, L. Tong, Crystal structure of 1-deoxy-D-xylulose 5-phosphate synthase, a crucial enzyme for isoprenoids biosynthesis. *J. Biol. Chem.* **282**, 2676–2682 (2007).
78. K. Olavarría, D. Valdés, R. Cabrera, The cofactor preference of glucose-6-phosphate dehydrogenase from *Escherichia coli*–Modeling the physiological production of reduced cofactors. *FEBS J.* **279**, 2296–2309 (2012).